





RESEARCH ARTICLE

Radiocarbon evidence over the apparent grand solar minimum around 400 BCE

Michael Dee¹ , Andrea Scifo¹ , Tarun Rohra¹, Jente Joosten¹, Margot Kuitems¹ , Wesley Vos¹, Sturt Manning^{2,3}  and Thorsten Westphal⁴

¹University of Groningen, Centre for Isotope Research, Groningen, 9747 AG, Netherlands, ²Cornell University, Classics Department, 120 Goldwin Smith Hall, Ithaca, NY 14853-0001, USA, ³Cornell University, Cornell Institute of Archaeology and Material Studies, McGraw Hall, Ithaca, NY 14853-0001, USA and ⁴University of Cologne, Laboratory of Dendroarchaeology, Department of Prehistoric Archaeology, Cologne, Germany

Corresponding author: Michael Dee; Email: m.w.dee@rug.nl

Received: 15 April 2024; **Revised:** 07 August 2024; **Accepted:** 12 September 2024; **First published online:** 13 February 2025

Keywords: grand solar minimum; radiocarbon; solar activity

Abstract

Grand solar minima are periods spanning from decades to more than a century during which solar activity is unusually low. A cluster of such minima occurred during the last millennium, as evidenced by reductions in the numbers of sunspots observed and coeval increases in cosmogenic isotope production. Prior to the period of instrumental records, natural archives of such isotopes are the only resources available for detecting grand solar minima. Here, we examine the period 433–315 BCE, which saw a sustained increase in the production of the cosmogenic isotope, radiocarbon. Our new time series of radiocarbon data ($\Delta^{14}\text{C}$), obtained on cellulose extracted from known-age oak tree rings from Germany, reveal that the rise in production that occurred at this time was commensurate with patterns observed over recent grand solar minima. Our data also enhance, and to a degree challenge, the accuracy of the international atmospheric radiocarbon record over this period.

Introduction

The temporal range of instrumental records is insufficient for a complete picture of the behavior of the Sun. Space-based observations of total irradiance and the dynamics of the solar wind first came onstream in 1978, and telescopic observations of sunspots peter out in the early 17th century. Thus, even with best current efforts, there are only four centuries of data (Clette and Lefèvre 2016; Eddy 1976; Hathaway 2010; Svalgaard and Schatten 2016). As a consequence, all long-term reconstructions of solar activity rely on proxy evidence from natural archives. The key raw data are cosmogenic isotope concentrations, principally ^{14}C (radiocarbon), preserved in dendrochronologically dated tree rings, and ^{10}Be and ^{36}Cl , trapped in ice cores (Beer 2000; Beer et al. 1988; Muscheler et al. 2007; Usoskin 2017). The initial data processing step involves converting these results, obtained at ground level, into true fluctuations in production in the upper atmosphere, using models of isotope transport and deposition. Over the longer term, account must also be taken of obfuscating variables such as the strength of the geomagnetic field. By correcting for all such factors, a function is derived called the solar modulation potential (SMP or Φ), which reveals the activity of the Sun over time via changes in cosmogenic isotope production (Beer 2000; Gleeson and Axford 1968; Masarik and Beer 1999; Muscheler et al. 2007).

In order to compare the utility of these cosmogenic isotopes for palaeosolar research, it is necessary to review their modes of production and deposition. The formation mechanisms of ^{14}C , ^{10}Be and ^{36}Cl are closely related but not identical. The nuclides are all predominantly generated in the lower stratosphere due to the ongoing incursion of high-energy ($>10^2$ MeV) galactic cosmic rays (GCR). ^{10}Be

atoms are largely the result of direct spallation of atmospheric oxygen (^{16}O) and nitrogen (^{14}N) nuclei and ^{36}Cl is generated by the spallation of argon (^{40}Ar or ^{36}Ar ; see Beer et al. 2012). However, due to its low concentration and the challenges involved in its measurement, ^{36}Cl is rarely used for fine-scaled profiling of solar activity, and it will also not be considered in this study. The most common production pathway for ^{14}C formation involves nitrogen capturing thermalized neutrons emanating from the primary cosmic ray bombardment: $^{14}\text{N}[n, p]^{14}\text{C}$ (Beer et al. 2012).

Under normal circumstances, the energy spectrum of the solar particle flux is too soft (of the order of keV rather than MeV) to instigate the spallation reactions necessary for cosmogenic isotope production (Masarik and Reedy 1995; Kovaltsov et al. 2012). In fact, the formation of these isotopes is roughly anti-correlated with solar output. This is because an increase in solar activity results in an intensification of the interplanetary magnetic field (IMF) carried by the solar wind, which in turn also compresses the geomagnetic field. The combined effect of these two processes is that high-energy GCR from deep space are more efficiently deflected away from the Earth, and hence cosmogenic isotope production falls. In this study the opposite scenario is examined, wherein declining solar output facilitates an increase in cosmogenic isotope production.

^{10}Be and ^{14}C have contrasting modes of deposition. Newly formed ^{10}Be is first adsorbed on aerosols, primarily sulfate particles (Morris 1991; Raisbeck and Yiou 1981) and ultimately deposited in ice. The actual amounts deposited in the ice are then mainly the result of “scavenging” by falling snow (Igarashi et al. 1998). Residence times in the atmosphere are thought to average around 1 year (Heikkilä et al. 2013). Analysis of ^{10}Be accumulation in the ice layers is complicated by volcanic activity, which enhance sulfate aerosol concentrations, and local “climatic impacts” that amount to site-specific variations in wind patterns, precipitation and surface disturbances (Baroni 2019; Heikkilä et al. 2013; Zheng et al. 2023). Furthermore, the complexity and expense of obtaining ^{10}Be data means annual sampling resolution is only rarely practicable (Paleari et al. 2022; Vonmoos et al. 2006). Results tend to be given as concentrations (atoms g^{-1}) for layers of a given core, although sometimes modelled estimates of the ^{10}Be flux are provided. As a result of these site-specific idiosyncrasies, most solar analyses amalgamate trends in ^{10}Be from multiple ice cores.

Upon formation, ^{14}C is first oxidized to ^{14}CO (Jöckel et al. 2003; Turnbull et al. 2009) and typically a few months pass before it is further oxidized to $^{14}\text{CO}_2$ (Jöckel et al. 2003). The atmospheric residence time of $^{14}\text{CO}_2$ is thought to range from 1 to 3 years (Scifo et al. 2019), and its final concentration at ground level, where it is taken up during photosynthesis and thus built into tree rings, is greatly dampened by carbon cycle processes. Atmospheric mixing of $^{14}\text{CO}_2$ is thorough, with the exception of a diminutive latitudinal gradient (Büntgen et al. 2018; Zhang et al. 2022). However, strong variation is observable over time in even pre-Industrial atmospheric concentrations. This is generally attributed to changes in oceanic dissolution, where the vast majority of $^{14}\text{CO}_2$ is deposited (Muscheler et al. 2007; Siegenthaler et al. 1983; Stuiver and Braziunas 1993). The Southern Hemisphere’s greater ocean surface, for instance, is thought to account for its $\sim 5\%$ deficit in atmospheric $^{14}\text{CO}_2$ levels relative to the Northern Hemisphere. Similarly, the reduced rate at which oceanic drawdown occurs during Glacial periods, has been proposed as an explanation for the marked difference in atmospheric concentrations of ^{14}C during the Pleistocene compared to the Holocene (Muscheler et al. 2008; Stocker and Wright 1996).

Atmospheric ^{14}C data from tree rings of known growth year are usually expressed as $\Delta^{14}\text{C}$, a ratio which includes a correction for radioactive decay, although the term originally proposed for pre-1950 samples was simply Δ (Stuiver and Polach 1977). High-precision data are now routinely obtained at $\sim 2\%$ and contain the temporal resolution of just one growing season. A minor component of “carry over” carbon from earlier years may be relevant in some circumstances (McDonald et al. 2019). Nonetheless, most of the legacy data that underlie the international reference curves are still averages obtained on 10-yearly or even 20-yearly blocks of tree rings. *Prima facie*, the newest curves (IntCal20, SHCal20) comprise single-year values over the last 5000 years but, prior to 1000 CE, these curves are reliant upon measurements of multiyear blocks of tree rings. Moreover, to calculate true changes in primary ^{14}C production, $\Delta^{14}\text{C}$ measurements on tree rings need to be passed through models of the global carbon cycle. Recently, the open-source tool `ticktack` became available (Zhang et al. 2022),

which allows users to upload $\Delta^{14}\text{C}$ values, select one of several published carbon cycle models, and calculate fluctuations relative to long-run average values. Whilst ^{10}Be data obviously do not require such carbon cycle corrections, ^{14}C records still form the backbone of most historical reconstructions of solar activity, for the following reasons. First, as described above, ^{10}Be is not immune to variations in local environmental conditions and the impact of geophysical events. Secondly, over the Holocene at least, ^{14}C archives are far more plentiful and exhibit a far greater geographical and temporal coverage than the ice cores. To elaborate, before the Common Era ^{10}Be is almost only available at decadal resolution or worse, meaning patterns of sub-centennial duration are virtually undetectable. More practically, the greater ease with which high-precision ^{14}C measurements can be obtained on annual samples is also a key advantage. This paper focuses on increases in $\Delta^{14}\text{C}$ that have occurred for periods of decades or more, and in particular the sustained rise in $\Delta^{14}\text{C}$ that is observed around 400 BCE (2349 cal BP).

A multi-decadal increase in SMP, derived from the analysis of cosmogenic isotope data, is usually interpreted as a grand solar minimum (GSM). GSM are extended periods, from decades to a couple of centuries, during which the magnetic activity of the sun is unusually weak (see Usoskin 2017; Usoskin et al. 2007). As a GSM progresses, the pattern observed in $\Delta^{14}\text{C}$ in the tree-ring archives is a combination of the rise in primary production and the gradual drawdown of the excess ^{14}C by the biosphere and oceans. Thus, a lag always exists between a return to “normal” magnetic activity on the Sun and the restoration of “normal” cosmogenic isotope levels in the atmosphere. This effect is manifest, albeit in a more extreme fashion, by the residual ^{14}C enrichment in the atmosphere after the cessation of atmospheric nuclear bomb testing in 1963 (Hua et al. 2013). Because of this delay, the exact duration of individual GSM is not a straightforward matter. To elaborate, the extent to which the decreasing part of the $\Delta^{14}\text{C}$ perturbation corresponds to reduced but gradually increasing solar activity, and how much simply reflects the gradual drawdown of excess ^{14}C in the atmosphere, remains unclear. Programs which filter the data through the carbon cycle, like *ticktack*, can be of help in making this distinction. For simplicity’s sake, in this study we use the timings given by Usoskin (2017) as approximations for the chronological positioning of recent GSM, which generally only traverse the ascending portion of the $\Delta^{14}\text{C}$ perturbation. These are as follows: Oort (990–1070 CE); Wolf (1270–1350 CE); Spörer (1390–1550 CE); Maunder (1640–1720 CE) and Dalton (1797–1828 CE).

In addition, prolonged enhancements in atmospheric ^{14}C can also be driven by environmental processes, especially by abrupt cooling events associated with increased ice cover and rapid declines in deepwater formation (Muscheler et al. 2008; Stocker and Wright 1996). Here, unless the equivalent period is robustly traversed by ^{10}Be data, the true cause of the elevation in ^{14}C may be difficult to discern.

In this paper, special attention is paid to the rise in atmospheric $\Delta^{14}\text{C}$ around 400 BCE. Few isotopic studies have focused on this period, though the profile has previously been attributed to a GSM (Nagaya et al. 2012; Usoskin et al. 2007). Indeed, it has even casually been referred to as the “Greek Minimum” (Wang et al. 2022), although perhaps “Platonic Minimum” would better distinguish it from the similarly proposed Homeric Minimum (ca. 800 BCE; Martin-Puertas et al. 2012). Here, new high-resolution $\Delta^{14}\text{C}$ data have been obtained to shed more light on this section of IntCal20, which is still mainly traversed by decadal data.

Methods

Physical and chemical pretreatment of samples

The wood sample obtained for this investigation was a subfossil oak (*Quercus* sp.) from the Elbe River in Germany, provided by the dendro archive of Curt-Engelhorn-Zentrum Archäometrie (CEZA) Mannheim. The sample was first cleaved along its annual growth rings using a steel blade. Subsamples ~100 mg in size were then prepared for α -cellulose extraction. The oak sample used to produce nearly all the data is shown in the Supplementary Information (SI).

The Centre for Isotope Research (CIO)'s routine α -cellulose procedure is described in detail elsewhere (Dee et al. 2020). In essence, it involves a series of acid ($\text{HCl}_{(\text{aq})}$), base ($\text{NaOH}_{(\text{aq})}$), and oxidation ($\text{NaClO}_{2(\text{aq})}$) steps in order to isolate the most intact polysaccharides (principally cellulose) from the whole wood sample. By the inclusion of known-age tree-ring samples in every pretreatment batch, and through participation in numerous interlaboratory comparisons (Bayliss et al. 2020; Kuitens et al. 2021; Wacker et al. 2020, Laboratory 15), CIO's α -cellulose protocol has proven to be exceptionally accurate. All the subsamples were subjected to said protocol. Thereafter, ~ 5 mg aliquots of the extracted cellulose were weighed into tin capsules, whereupon they were combusted in an Elemental Analyser (Elementar Vario Isotope Cube) coupled to an Isotope Ratio Mass Spectrometer (IsoPrime 100) and a custom-made cryogenic collection system. The latter apparatus traps the $\text{CO}_{2(\text{g})}$ liberated from each sample and, after manual transfer, it is subsequently reduced to $\text{C}_{(\text{s})}$ (graphite) using a stoichiometric excess of $\text{H}_{2(\text{g})}$ and an $\text{Fe}_{(\text{s})}$ catalyst. The graphite was then pressed into cathodes for radioisotope measurement on a Micadas 200 kV accelerator mass spectrometer (Aerts-Bijma et al. 2021; Dee et al. 2020).

Results and discussion

The new ^{14}C data

Table S1 (SI) shows the 57 ^{14}C data obtained on the tree rings in both conventional radiocarbon age (CRA, yr BP) and $\Delta^{14}\text{C}$ (‰) formats. The set of annual samples is spread over the period 426–325 BCE. However, only 3 years are covered between 426–414; only 6 years are covered between 394–367; and thereafter the data are biennial. A total of 5 samples were taken through as full pretreatment duplicates, the results for all of which passed the χ^2 test for statistical congruence at 95% probability (see Table S2, SI; Ward and Wilson 1978). By averaging those 5 duplicates a new set of 52 datapoints was obtained for the period around 400 BCE and subjected to the following analyses.

Comparisons with IntCal20

The new data set is of immediate value. It traverses the ascending portion of the $\Delta^{14}\text{C}$ perturbation in the Northern Hemisphere calibration curve (IntCal20, Reimer et al. 2020) commencing around 400 BCE (2349 cal BP), but in far greater detail than ever previously achieved. Figure 1a shows the data currently underlying this period of IntCal20. The time series comprises no single-year data but only averages over multiyear blocks of tree rings. Curiously, the IntCal20 curve, a smoothed function through this data, exhibits a shoulder around 380 BCE (2329 cal BP), yet the basis for this is not immediately apparent in the raw data. Our new results (Figure 1b) generally agree with the existing record, overlying it closely in the early period but not peaking as high as the constituent data sets of IntCal20. Ours also show little evidence of a shoulder around 380 BCE (2329 cal BP). The overall difference between the smoothed IntCal20 record and our $\Delta^{14}\text{C}$ data is $-3.4 \pm 0.4\text{‰}$ (or $+26.2 \pm 3.3$ ^{14}C yrs). It is worth noting that an apparently minor difference like this, if corroborated by other sources, is likely to have significant implications for the calibration of ^{14}C dates over this time period.

Comparisons with ^{14}C production over established grand solar minima

In order to compare the excess $\Delta^{14}\text{C}$ produced around 400 BCE, we have used *ticktack*. All the settings employed in our *ticktack* analysis are given in Table S4 of the SI. Figure 2 shows the program estimates that this particular rise commenced around 410 BCE (2359 cal BP) and lasted 78.1 years, and involved an increase in ^{14}C production rate of around 0.3 atoms cm^2 s^{-1} per year above normal (Figure 2a, lower panel) or of total of 23 atoms cm^2 s^{-1} per year excess production across the whole 78.1 year period (Q parameter, Figure 2b). Assuming a sinusoidal rise and fall in $\Delta^{14}\text{C}$ due to the

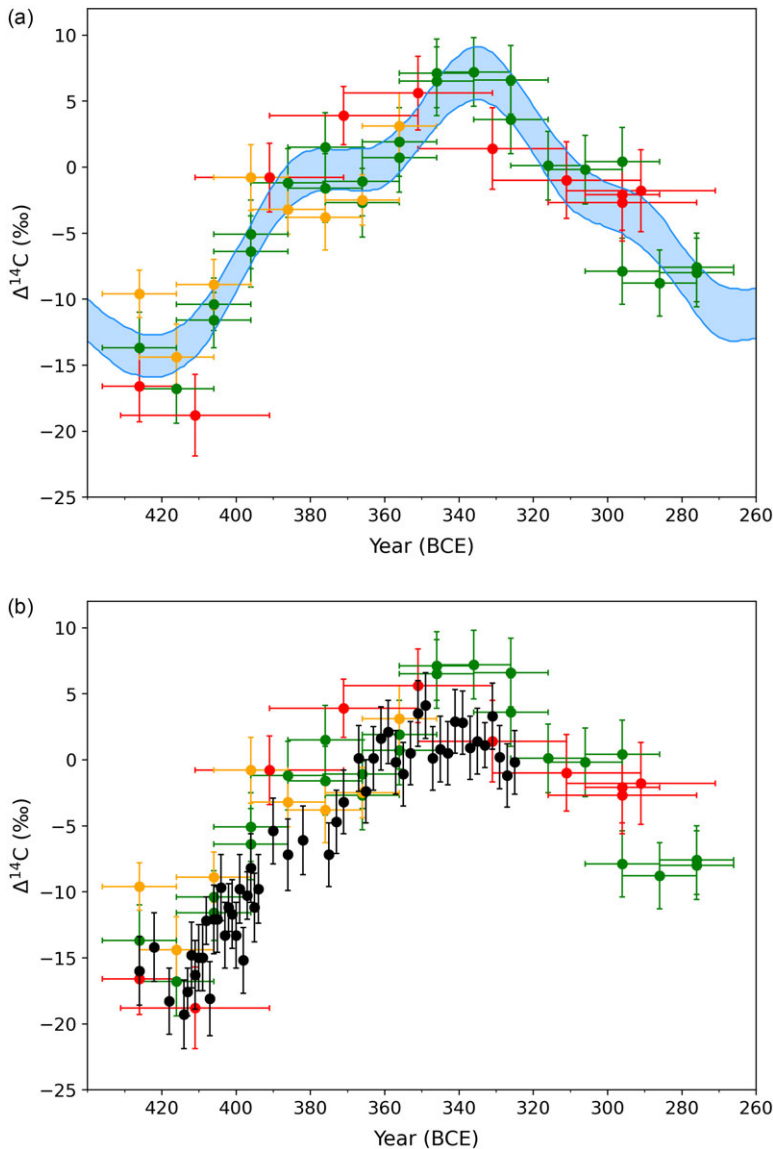


Figure 1. (a) The raw data underlying IntCal20 [see Reimer et al. (2020), Seattle (QL, green), Belfast (UB, red), Irvine (UCI, orange)], and the smoothed IntCal20 curve ($\pm 1\sigma$ envelope, blue). (b) Single-year data from this study [Groningen (GrM, black)] superimposed on the raw IntCal20 data.

Schwabe cycle, *ticktack* is also able to interpolate the data and determine the most probable number of these phase changes. In this case, the program estimates that the rise lasted approximately 7 full cycles. It should be noted, as stated above, that our data set does not cover every year (Table S1 SI), and a number of independent time series should really be combined in order to shore up the observed patterns. The precise date of the onset of the GSM, for example, would benefit from increased data density in the decades prior to 410 BCE.

Nonetheless, there is a compelling similarity in the duration and magnitude of the increase in $\Delta^{14}\text{C}$ around 400 BCE and the Oort, Wolf and Maunder minima, especially. As expected, *ticktack* also estimates that the production rate returns to normal levels (~ 330 BCE) some years before the $\Delta^{14}\text{C}$ signal drops down to the pre-GSM levels (~ 270 BCE, see Figures 1a and 2a). The Spörer and Dalton

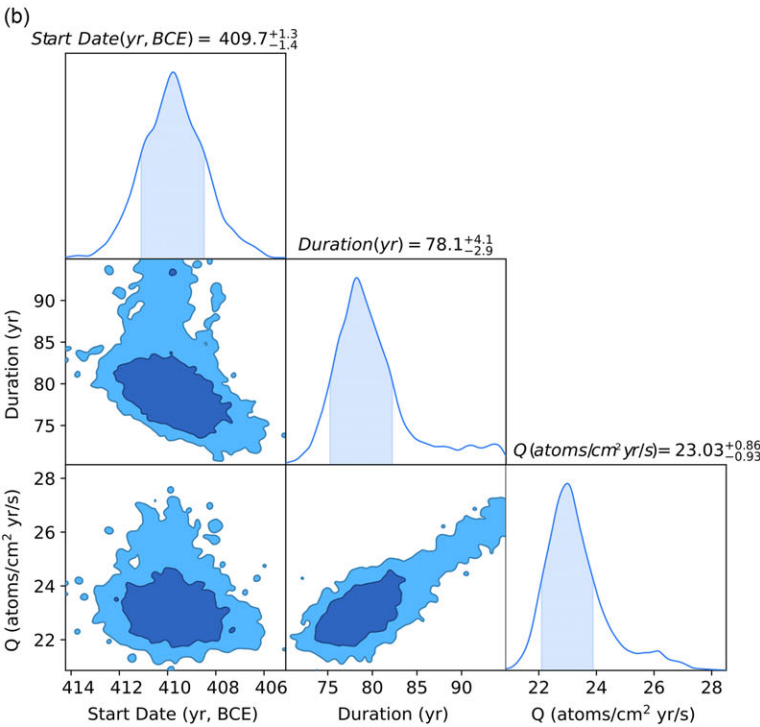
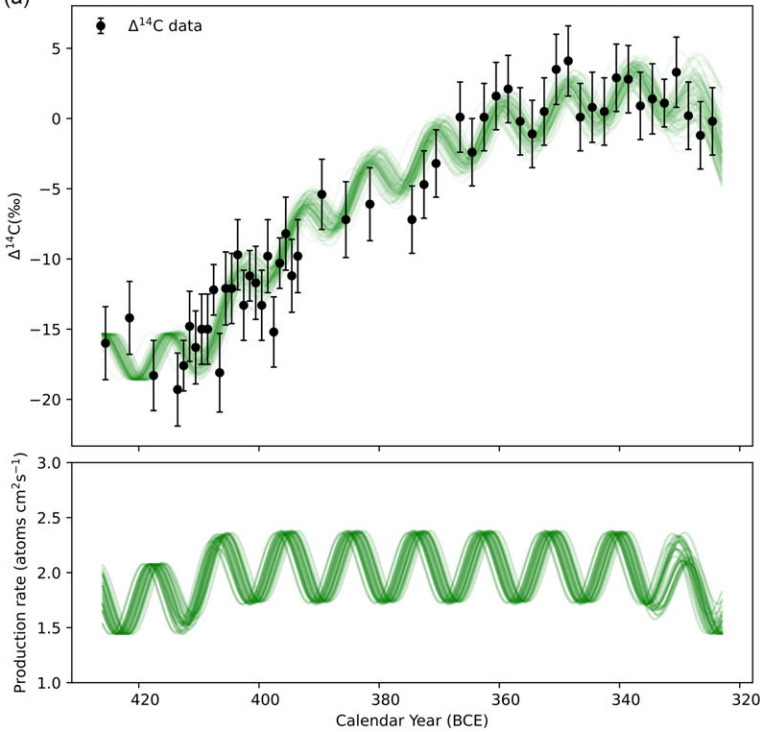


Figure 2. New annual $\Delta^{14}C$ data over the period around 400 BCE analyzed using the *ticktack* python package. (a) The profile of the rise in $\Delta^{14}C$ production interpolated by the program's *simple_sinusoid* Bayesian inference model (class object, *sf* = *SingleFitter*). (b) Cornerplots from *ticktack* for the rise in 400 BCE showing the 68% (dark blue) and 95% (light blue) highest posterior density estimates for start date, duration and area (overall excess ^{14}C production). Specifications for *ticktack* analysis available in Table S4, SI.

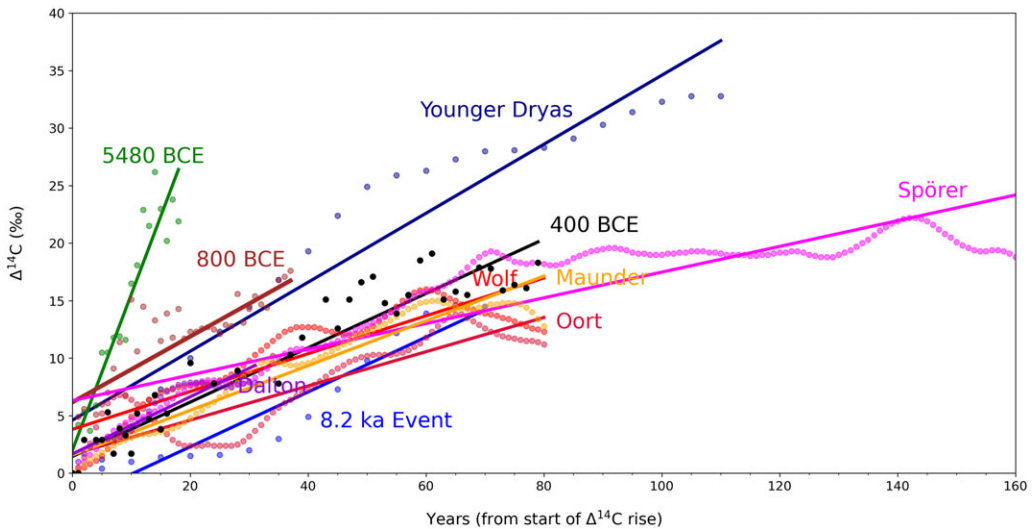


Figure 3. $\Delta^{14}\text{C}$ time series over various solar and environmental events (see SI for raw data). The five established GSM are shown, as well as profiles over two established environmental events (Younger Dryas and 8.2 ka Event, Reimer et al. 2020). Shown also are our new data over 400 BCE, and two profiles over 800 BCE (Jull et al. 2018) and 5480 BCE (Miyake et al. 2017), where the $\Delta^{14}\text{C}$ increases have also been attributed to reduced solar activity. The general trend in each dataset is highlighted by linear polynomials.

Minima do not replicate our results so closely but these GSM are known to be somewhat anomalous. In fact, GSM have previously been classed into Maunder-like (shorter) and Spörer-like (longer) minima (Schüssler et al. 1997; Sokoloff 2004; Usoskin 2017), and the true nature of the Dalton (very short) minimum is still being debated (Frick et al. 1997; Usoskin 2017).

Comparisons with other periods of increasing ^{14}C production

Despite the similarity of the $\Delta^{14}\text{C}$ profile over 400 BCE with several established GSM, the possibility the sudden uplift has a totally different origin altogether must also be considered. As previously discussed, increases in production may also be the result of environmental (carbon cycle) processes. Figure 3 shows the periods over which some pronounced rises in the IntCal20 $\Delta^{14}\text{C}$ dataset occurred during the Holocene and Late Pleistocene for which explanations have already been widely agreed.

It is clear from Figure 3 that these two intense cooling events are associated with rises in $\Delta^{14}\text{C}$ that are of a similar rate and duration to GSM. To express this quantitatively, the gradients (with 1 σ uncertainties) of the linear polynomials of the established five GSM range from 0.11 ± 0.00 (Spörer) to $0.25 \pm 0.02 \text{ ‰ yr}^{-1}$ (Dalton), and the corresponding values for the 8.2 ka Event and YD are 0.24 ± 0.02 and $0.30 \pm 0.02 \text{ ‰ yr}^{-1}$ (IntCal 20, Reimer et al. 2020, Tables S5 and S6, SI), respectively. However, on the time scales relevant to this study the sparsity of ^{10}Be data make it difficult to reliably discriminate between GSM and environmental events. As shown in Figure 3, two further $\Delta^{14}\text{C}$ profiles have recently been published which the authors have connected with reduced solar activity (see Figure 3, 5480 BCE, Miyake et al. 2017, Table S7, SI; 800 BCE, Jull et al. 2018, Table S8, SI). Presently, historical information and data from other climatic proxies coincident with these events is probably the most effective way of favoring either an environmental or a solar cause. It is also worth highlighting that the rise observed in 5480 BCE appears not to match either the trend of the established GSM or the known environmental events examined in this study. Indeed, it exhibits an anomalously steep increase ($1.36 \pm$

0.11 %_o yr⁻¹) which, if it were to have had an environmental origin, would need to have relate to an extreme and as yet unknown climatic downturn. It seems more probable that this rapid rise was the result of a sudden and ephemeral decline in solar activity of a mechanism not yet fully understood. At the time of publication, the authors simply described the data set as evidence of an “unprecedented anomaly in solar activity.”

Conclusions

Sustained rises in atmospheric $\Delta^{14}\text{C}$ concentration are generally regarded as evidence of GSM, which enable greater ^{14}C production, or intense cold events which inhibit oceanic drawdown of atmospheric $^{14}\text{CO}_2$. Further explanations, including poorly understood types of solar behavior, remain possible. Ascribing a prolonged increase to one of these potential causes is currently challenging. Here, we present one of the most detailed data sets published to date for the increase in $\Delta^{14}\text{C}$ around 400 BCE. Whilst our data do generally overlie the current Northern Hemisphere radiocarbon reference curve (IntCal20), they are somewhat more depleted and do not reproduce all of its features. In terms of the origin of the rate of increase in $\Delta^{14}\text{C}$ around 400 BCE, our data set is consistent with all 5 established GSM during the last millennium, and the duration of the increase and the excess ^{14}C produced appear to be almost identical to the Oort and Wolf minima. Furthermore, no extremely cold period during the 5th and 4th centuries BCE is historically documented nor evident in available climate proxies (e.g. Büntgen et al. 2011; Gillreath-Brown et al. 2024; Manning 2022; Sinha et al. 2019). In the absence of detailed annual ^{10}Be data, which may be able to answer this question more definitively, the most parsimonious explanation still appears to be a GSM.

Supplementary material. To view supplementary material for this article, please visit <https://doi.org/10.1017/RDC.2024.132>

Data availability. All of the isotope data used for the analyses in this study are available in the Supplementary Information (SI) of this article. The previously published $\Delta^{14}\text{C}$ data are given in Miyake et al. (2017), Jull et al. (2018) and Reimer et al. (2020).

Acknowledgments. This work was supported by a European Research Council grant (ECHOES, 714679).

Declaration. The authors declare no competing interests.

References

- Aerts-Bijma AT, Paul D, Dee MW, Palstra SWL and Meijer HAJ (2021) An independent assessment of uncertainty for radiocarbon analysis with the new generation high-yield accelerator mass spectrometers. *Radiocarbon* **63**(1), 1–22. <https://doi.org/10.1017/RDC.2020.101>
- Baroni M (2019) Isotope archiving in ice cores. In Miyake F, Usoskin I and Poluianov S (eds), *Extreme Solar Particle Storms: The Hostile Sun*. Bristol: IOP Publishing, 4/36–4/31. <https://iopscience.iop.org/book/edit/978-0-7503-2232-4>
- Bayliss A, Marshall P, Dee MW, Friedrich M, Heaton TJ and Wacker L (2020) IntCal20 tree rings: An archaeological SWOT analysis. *Radiocarbon* **62**(4), 1045–1078. <https://doi.org/10.1017/RDC.2020.77>
- Beer J (2000) Long-term indirect indices of solar variability. *Space Science Reviews* **94**, 53–66. <https://link.springer.com/article/10.1023/A:1026778013901>
- Beer J, McCracken K and von Steiger R (2012) *Cosmogenic Radionuclides*. Berlin and Heidelberg: Springer-Verlag, 133–291.
- Beer J, Siegenthaler U, Bonani G, Finkel RC, Oeschger H, Suter M and Wölfli W (1988) Information on past solar activity and geomagnetism from ^{10}Be in the Camp Century ice core. *Nature* **331**, 675–679. <https://doi.org/10.1038/331675a0>
- Büntgen U, Tegel W, Nicolussi K, McCormick M, Frank D, Trouet V, Kaplan JO, Herzig F, Heussner K-U, Wanner H, Luterbacher J and Esper J (2011) 2500 years of European climate variability and human susceptibility. *Science* **331**, 578–582. <https://doi.org/10.1126/science.1197175>
- Büntgen U, Wacker L, Galván JD, Arnold S, Arseneault D, Baillie M, Beer J, Bernabei M, Bleicher N, Boswijk G, Bräuning A, Carrer M, Ljungqvist FC, Cherubini P, Christl M, Christie DA, Clark PW, Cook ER, D’Arrigo R, Davi N, Eggertsson Ó, Esper J, Fowler AM, Gedalof Z, Gennaretti F, Grießinger J, Grissino-Mayer H, Grudd H, Gunnarson BE, Hantemirov R, Herzig F, Hessl A, Heussner K-U, Jull AJT, Kukarskih V, Kirilyanov A, Kolář T, Krusic PJ, Kyncl T, Lara A, LeQuesne C, Linderholm HW, Loader NJ, Luckman B, Miyake F, Myglan VS, Nicolussi K, Oppenheimer C, Palmer J, Panyushkina I, Pederson N, Rybníček M, Schweingruber FH, Seim A, Sigl M, Churakova Sidorova O, Speer JH, Synal H-A, Tegel W, Treydte K, Villalba R, Wiles G, Wilson R, Winship LJ, Wunder J, Yang B and Young GHF (2018) Tree rings reveal globally coherent signature of

- cosmogenic radiocarbon events in 774 and 993 CE. *Nature Communications* **9**, 3605. <https://doi.org/10.1038/s41467-018-06036-0>
- Clette F and Lefèvre L (2016) The new sunspot number: Assembling all corrections. *Solar Physics* **291**, 2629–2651. <https://link.springer.com/article/10.1007/s11207-016-1014-y>.
- Dee MW, Palstra SWL, Aerts-Bijma AT, Bleeker MO, de Bruijn S, Ghebru F, Jansen HG, Kuitens M, Paul D, Richie RR, Spriensma JJ, Scifo A, Van Zonneveld D, Verstappen-Dumoulin BMAA, Wietzes-Land P and Meijer HAJ (2020) Radiocarbon dating at Groningen: New and updated chemical pretreatment procedures. *Radiocarbon* **62**(1), 63–74. <https://doi.org/10.1017/RDC.2019.101>
- Eddy JA (1976) The Maunder Minimum. *Science* **192**(4245), 1189–1202. <https://doi.org/10.1126/science.192.4245.1189>
- Frick P, Galyagin D, Hoyt DV, Nesme-Ribes E, Schatten KH, Sokoloff D and Zakharov V (1997) Wavelet analysis of solar activity recorded by sunspot groups. *Astronomy and Astrophysics* **328**, 670–681. <https://articles.adsabs.harvard.edu/pdf/1997A%26A...328..670F>
- Gillreath-Brown A, Bocinsky RK and Kohler TA (2024) A low-frequency summer temperature reconstruction for the United States Southwest, 3000 BC–AD 2000. *The Holocene*. <https://doi.org/10.1177/09596836231219482>
- Gleeson LJ and Axford WI (1968) Solar modulation of galactic cosmic rays. *Astrophysical Journal* **154**, 1011–1018. <https://link.springer.com/article/10.12942/lrsp-2013-3>
- Hathaway DH (2010) The solar cycle. *Living Reviews in Solar Physics* **7**(1), 1–65. <https://link.springer.com/article/10.1007/lrsp-2015-4>
- Heikkilä U, Beer J, Abreu JA and Steinhilber F (2013) On the atmospheric transport and deposition of the cosmogenic radionuclides (^{10}Be), a review. *Space Science Reviews* **176**(1–4), 321–332. <https://link.springer.com/article/10.1007/s11214-011-9838-0>
- Hua Q, Barbetti M and Rakowski AZ (2013) Atmospheric radiocarbon for the period 1950–2010. *Radiocarbon* **55**(4), 2059–2072. https://doi.org/10.2458/azu_js_rc.v55i2.16177
- Igarashi Y, Hirose K and Otsuji-Hatori M (1998) Beryllium-7 deposition and its relation to sulfate deposition. *Journal of Atmospheric Chemistry* **29**(3), 217–231. <https://link.springer.com/article/10.1023/A:1005921113496>
- Jöckel P, Brenninkmeijer CAM, Lawrence MG and Siegmund P (2003) The detection of solar proton produced ^{14}C . *Atmospheric Chemistry and Physics* **3**, 999–1005. <https://acp.copernicus.org/articles/3/999/2003/>
- Jull AJT, Panyushkina I, Miyake F, Masuda K, Nakamura T, Mitsutani T, Lange TE, Cruz RJ, Baisan C, Janovics R, Varga T and Molnár M (2018) More rapid ^{14}C excursions in the tree-ring record: A record of different kind of solar activity at about 800 BC? *Radiocarbon* **60**(4), 1237–1248. <https://doi.org/10.1017/RDC.2018.53>
- Kovaltsov GA, Mishev A and Usoskin IG (2012) A new model of cosmogenic production of radiocarbon ^{14}C in the atmosphere. *Earth and Planetary Science Letters* **337–338**, 114–120. <https://doi.org/10.1016/j.epsl.2012.05.036>
- Kuitens M, Wallace BL, Lindsay C, Scifo A, Doeve P, Jenkins K, Lindauer S, Erdil P, Ledger PM, Forbes V, Vermeeren C, Friedrich R and Dee MW (2021) Evidence for European presence in the Americas in AD 1021. *Nature* **601**, 388–391. <https://doi.org/10.1038/s41586-021-03972-8>
- Manning SW (2022) Climate, environment, and resources. In von Reden S (ed), *The Cambridge Companion to the Ancient Greek Economy*. Cambridge: Cambridge University Press, 373–391. <https://doi.org/10.1017/9781108265249.025>
- Martin-Puertas C, Matthes K, Brauer A, Muscheler R, Hansen F, Petrick C, Aldahan A, Possnert G and van Geel B (2012) Regional atmospheric circulation shifts induced by a grand solar minimum. *Nature Geoscience* **5**, 397–401. <https://doi.org/10.1038/ngeo1460>
- Masarik J and Reedy RC (1995) Terrestrial cosmogenic-nuclide production systematics calculated from numerical simulations. *Earth and Planetary Science Letters* **136**(3–4), 381–395. [https://doi.org/10.1016/0012-821X\(95\)00169-D](https://doi.org/10.1016/0012-821X(95)00169-D)
- Masarik J and Beer J (1999) Simulation of particle fluxes and cosmogenic nuclide production in the Earth's atmosphere. *Journal of Geophysical Research* **104**, 12099–12111. <https://doi.org/10.1029/2008JD010557>
- McDonald L, Chivall D, Miles D and Bronk Ramsey C (2019) Seasonal variations in the ^{14}C content of tree rings: Influences on radiocarbon calibration and single-year curve construction. *Radiocarbon* **61**(1), 185–194. <https://doi.org/10.1017/RDC.2018.64>
- Miyake F, Jull AJT, Panyushkina IP, Wacker L, Salzer M, Baisan CH, Lange T, Cruz R, Masuda K and Nakamura T (2017) Large ^{14}C excursion in 5480 BC indicates an abnormal sun in the mid-Holocene. *Proceeding of the National Academy of Sciences* **114**(5), 881–884. <https://doi.org/10.1073/pnas.1613144114>
- Morris JD (1991) Applications of cosmogenic ^{10}Be to problems in the earth sciences. *Annual Review of Earth and Planetary Sciences* **19**, 313–350. <https://doi.org/10.1146/annurev.ea.19.050191.001525>
- Muscheler R, Joos F, Beer J, Muller SA, Vonmoos M and Snowball I (2007) Solar activity during the last 1000 yr inferred from radionuclide records. *Quaternary Science Reviews* **26**, 82–97. <https://doi.org/10.1016/j.quascirev.2006.07.012>
- Muscheler R, Kromer B, Björck S, Svensson A, Friedrich M, Kaiser KF and Southon J (2008) Tree rings and ice cores reveal ^{14}C calibration uncertainties during the Younger Dryas. *Nature Geoscience* **1**(4), 263–267. <https://doi.org/10.1038/ngeo128>
- Nagaya K, Kitazawa K, Miyake F, Masuda K, Muraki Y, Nakamura T, Miyahara H and Matsuzaki H (2012) Variation of the Schwabe Cycle length during the grand solar minimum in the 4th century BC deduced from radiocarbon content in tree rings. *Solar Physics* **280**(1), 223–236. <https://link.springer.com/article/10.1007/s11207-012-0045-2>
- Paleari CI, Mekhaldi F, Erhardt T, Zheng M, Christl M, Adolphi F, Hörhold M and Muscheler R (2022) Evaluating the 11-year solar cycle and short-term ^{10}Be deposition events with novel excess water samples from the East Greenland Ice-core Project (EGRIP). *Climate of the Past* **19**(11), 2409–2422. <https://doi.org/10.5194/cp-19-2409-2023>

- Raisbeck GM and Yiou F (1981) Cosmogenic $^{10}\text{Be}/^{7}\text{Be}$ as a probe of atmospheric transport processes. *Geophysical Research Letters* **8**(9), 1015–1018. <https://doi.org/10.1029/GL008i009p01015>
- Reimer PJ, Austin WEN, Bard E, Bayliss A, Blackwell PG, Ramsey CB, Butzin M, Cheng H, Edwards RL, Friedrich M, Grootes P, Guilderson T, Hajdas I, Heaton T, Hogg A, Hughen K, Kromer B, Manning S, Muscheler R, Palmer J, Pearson C, van der Plicht J, Reimer R, Richards D, Scott E, Southon J, Turney C, Wacker L, Adolphi F, Büntgen U, Capano M, Fahrni S, Fogtmann-Schulz A, Friedrich R, Köhler P, Kudsk S, Miyake F, Olsen J, Reinig F, Sakamoto M, Sookdeo A and Talamo S (2020) The IntCal20 Northern Hemisphere radiocarbon age calibration curve (0–55 cal kBP). *Radiocarbon* **62**(4), 725–757. <https://doi.org/10.1017/RDC.2020.41>.
- Schüssler M, Schmitt D and Ferriz-Mas A (1997) Long-term variation of solar activity by a dynamo based on magnetic flux tubes. In Schmieder B, del Toro Iniesta JC and Vázquez M (eds), *1st Advances in Solar Physics Euroconference: Advances in the Physics of Sunspots*, *Astronomical Society of the Pacific, San Francisco*. ASP Conference Series 118, 39–44. <https://adsabs.harvard.edu/full/1997ASPC..118...39S>
- Scifo A, Kuitems M, Neocleous A, Pope BJS, Miles D, Jansma E, Döve P, Smith AM, Miyake F and Dee MW (2019) Radiocarbon production events and their potential relationship with the Schwabe cycle. *Scientific Reports* **9**(1), 17056. <https://doi.org/10.1038/s41598-019-53296-x>
- Siegenthaler U (1983) Uptake of excess CO_2 by an outcrop-diffusion model of the ocean. *Journal of Geophysical Research* **88**(6), 3599–3608. <https://doi.org/10.1029/JC088iC06p03599>
- Sinha A, Kathayat G, Weiss H, Li H, Cheng H, Reuter J, Schneider AW, Berkelhammer M, Adali SF, Stott LD and Edwards RL (2019) Role of climate in the rise and fall of the Neo-Assyrian Empire. *Science Advances* **5**, eaax6656. <https://doi.org/10.1126/sciadv.aax6656>
- Sokoloff D (2004) The Maunder Minimum and the solar dynamo. *Solar Physics* **224**, 145–152. <https://link.springer.com/article/10.1007/s11207-005-4176-6>
- Stocker TF and Wright DG (1996) Rapid changes in ocean circulation and atmospheric radiocarbon. *Paleoceanography* **11**(6), 773–795. <https://doi.org/10.1029/96PA02640>
- Stuiver M and Braziunas SF (1993) Modeling atmospheric ^{14}C influences and ^{14}C ages of marine samples to 10,000 BC. *Radiocarbon* **35**(1), 137–189. <https://doi.org/10.1017/S0033822200013874>
- Stuiver M and Polach H (1977) Reporting of ^{14}C data. *Radiocarbon* **19**(3), 355–363. <https://doi.org/10.1017/S0033822200003672>
- Svalgaard L and Schatten KH (2016) Reconstruction of the Sunspot Group Number: The backbone method. *Solar Physics* **291**, 2653–2684. <https://link.springer.com/article/10.1007/s11207-015-0815-8>
- Turnbull J, Rayner P, Miller J, Naegler T, Ciaia P and Cozic A (2009) On the use of $^{14}\text{CO}_2$ as a tracer for fossil fuel CO_2 : Quantifying uncertainties using an atmospheric transport model. *Journal of Geophysical Research* **114**, 1–13. <https://doi.org/10.1029/2009JD012308>
- Usoskin I (2017) A history of solar activity over millennia. *Living Reviews in Solar Physics* **14**(3), 1–97. <https://link.springer.com/article/10.1007/s41116-017-0006-9>
- Usoskin I, Solanki SK and Kovaltsov GA (2007) Grand minima and maxima of solar activity: New observational constraints. *Astronomy and Astrophysics* **471**, 301–309. <https://doi.org/10.1051/0004-6361:20077704>
- Vonmoos M, Beer J and Muscheler R (2006) Large variations in Holocene solar activity: Constraints from ^{10}Be in the Greenland Ice Core Project. *Journal of Geophysical Research* **111**(A10), 1–14. <https://doi.org/10.1029/2005JA011500>
- Wacker L, Scott EM, Bayliss A, Brown D, Bard E, Bollhalder S, Friedrich M, Capano M, Cherkinsky A, Chivall D, Culleton BJ, Dee MW, Friedrich R, Hodgins GWL, Hogg A, Kennett DJ, Knowles TDJ, Kuitems M, Lange TE, Miyake F, Nadeau M-J, Nakamura T, Naysmith JP, Olsen J, Omori T, Petchey F, Philippsen B, Bronk Ramsey C, Ravi Prasad GV, Seiler M, Southon J, Staff R and Tuna T (2020) Findings from an in-depth annual tree-ring radiocarbon intercomparison. *Radiocarbon* **62**(4), 873–882. <https://doi.org/10.1017/RDC.2020.49>
- Wang N, Shen C, Ding P, Ding X, Liu K, Sun W, Chen X, Deng W and Wei G (2022) Ocean circulation and climate variability in the northern South China Sea during the Greek Minimum derived from coral $\Delta^{14}\text{C}$ and Sr/Ca records. *Palaeogeography, Palaeoclimatology, Palaeoecology* **607**, 111276. <https://doi.org/10.1016/j.palaeo.2022.111276>
- Ward GK and Wilson SR (1978) Procedures for comparing and combining radiocarbon age determinations: A critique. *Archaeometry* **20**, 19–31. <https://doi.org/10.1111/j.1475-4754.1978.tb00208.x>
- Zhang Q, Sharma U, Dennis JA, Scifo A, Kuitems M, Büntgen U, Owens MJ, Dee MW and Pope BJS (2022) Modelling cosmic radiation events in the tree-ring radiocarbon record. *Proceedings of the Royal Society A* **478**(2266), 20220497. <https://doi.org/10.1098/rspa.2022.0497>
- Zheng M, Adolphi F, Paleari C, Tao Q, Erhardt T, Christl M, Wu M, Lu Z, Hörhold M, Chen P and Muscheler R (2023) Solar, atmospheric, and volcanic impacts on ^{10}Be depositions in Greenland and Antarctica during the last 100 years. *Journal of Geophysical Research: Atmospheres* **128**, e2022JD038392. <https://doi.org/10.1029/2022JD038392>

Cite this article: Dee M, Scifo A, Rohra T, Joosten J, Kuitems M, Vos W, Manning S, and Westphal T (2025). Radiocarbon evidence over the apparent grand solar minimum around 400 BCE. *Radiocarbon* **67**, 265–274. <https://doi.org/10.1017/RDC.2024.132>